Marine Pollution Bulletin 196 (2023) 115583

Contents lists available at ScienceDirect

Marine Pollution Bulletin

journal homepage: www.elsevier.com/locate/marpolbul

Plastitar in the Mediterranean Sea: New records and the first geochemical characterization of these novel formations

Francesco Saliu [a,*], Montserrat Compa [b], Alessandro Becchi [a], Marina Lasagni [a], Elena Collina [a], Arianna Liconti [c,d], Enzo Suma [e], Salud Deudero [b], Daniele Grech [f], Giuseppe Suaria [g]

[a] Earth and Environmental Science Department, University of Milano Bicocca, Piazza della Scienza 1, 20126 Milano, Italy
[b] Centro Oceanográfico de Baleares, (IEO, CSIC), Muelle de Poniente s/n, 07015 Mallorca, Spain
[c] OutBe SRL, Genova, Italy
[d] MBA, The Marine Biological Association, The Laboratory, Citadel Hill, Plymouth PL1 2PB, United Kingdom
[e] Archeoplastica, Italy
[f] IMC - International Marine Centre, Loc. Sa Mardini, 09170, Torregrande, Oristano, Italy
[g] CNR-ISMAR, Consiglio Nazionale delle Ricerche, Istituto di Scienze Marine, Pozzuolo di Lerici, 19032 La Spezia, Italy

ARTICLE INFO

Keywords:
Microplastics
Plastitar
Marine pollution
Plasticrust
Plastiglomerates
Mediterranean Sea

ABSTRACT

A new geological formation consisting of plastic debris admixed to petroleum oil residue, termed "plastitar", has been recently described in the Canary Islands. Here, we report its widespread occurrence across the Mediterranean coast and new insights into its biogeochemical composition. Specifically, we found marked differences in the diagenetic stable indicator profiles, suggesting a heterogeneous seeps provenance. Moreover, the 801 plastic particles found in the 1372 g of tar surveyed, with a maximum concentration of 2.0 items/g, showed interesting patterns in the tar mat, with nurdles predominantly layered in the external of the tar mat and lines in the inner core. Overall, the collected observation suggests that tar entraps plastics through a stepwise process and is a sink for them.

1. Introduction

The marine environment is increasingly exposed to threats caused by anthropogenic activities such as ocean acidification, global warming, raising levels of persistent organic pollutants and appearance of novel entities/emerging contaminants (Crain et al., 2008). Among these, plastic pollution has emerged as one of the most pervasive issues of our times (Eriksen et al., 2023).

Plastic is now so abundant and widespread in the natural environment that it has been proposed as a stratigraphic indicator of the Anthropocene (Zalasiewicz et al., 2016). More recently, plastic was proposed as a marker of the upper subdivision of a new geological stage: the Plasticene (Rangel-Buitrago et al., 2022). Plastics are indeed interacting with the geological cycle in many ways, and new geological formations are being increasingly reported in the scientific literature (e.g., De-la-Torre et al., 2021, 2022; Santos et al., 2022; Goswami and Bhadury, 2023). The so-called "Detriplastic rocks" (cf. Rangel-Buitrago et al., 2022) combine plastics in all sizes and shapes with solid particles (gravel, sand, silt, and clay) derived from pre-existing rocks by mechanical and chemical weathering. The leading example of this type of geological formations corresponds to plastiglomerates, first reported by Corcoran et al. (2014), which are composed of rock fragments, sand grains, plastic debris, and organic materials (i.e., shells, wood, and/or coral debris) held together by a plastic matrix. Other examples include pyroplastics (Turner et al., 2019), plasticrusts (Gestoso et al., 2019) and plastitar (Domínguez-Hernández et al., 2022).

Plastitar was first described in the Canary Islands (Spain) by Domínguez-Hernández et al. (2022), and was defined as an agglomerate of tar and plastics (mainly microplastics), which are amalgamated and attached to a rock surface and sometimes accompanied by the presence of small pieces of wood, glass, rocks, and sediments. Analyses of this formation indicated that it was substantially composed by an association of tar with plastic debris in the meso (25–5 mm) and micro (>5 mm) size range.

A previous report explicitly mentioning a clear association between stranded oil derived products with plastics was provided by Shiber in 1987, who reported that plastic pellets on Spanish Mediterranean beaches often had traces of tar on them, suggesting their close association

* Corresponding author.
E-mail address: francesco.saliu@unimib.it (F. Saliu).

https://doi.org/10.1016/j.marpolbul.2023.115583
Received 30 June 2023; Received in revised form 16 September 2023; Accepted 21 September 2023
Available online 26 September 2023

with beached tar. The same author reported similar observation in Kuwait (Shiber, 1989) and in Lebanon (Shiber and Barralesrienda, 1991). Turner and Holmes (2011), reported the occurrence of plastic production pellets embedded in tar deposits on rocks in Malta.

Regarding the plastitar genesis Domínguez-Hernández et al. (2022), suggested that the tar material was transported onshore by marine currents and then layered on the rocks. The tar in its initial form is oily but when exposed to UV light and warm temperature it faces a continuous circadian cycle of hardening and softening (caused by the different UV-light exposition and temperature at day and night). During this cycle, the tar admixes the plastic particles floating on the sea surface that are carried onshore by the tide or waves and settled on the top of the tar in the following days/weeks/months after the tar deposition, ultimately building a layered structure. At the very end of this formation process, the evaporation of the light weight and volatile components and the solidification of the high molecular weight fraction lead to a solid structure attached to coastal rocks and agglomerating a variety of materials: wood, glass, sand, and plastics. Since these agglomerates differ from other formations previously described in the literature (e.g., plastiglomerates, pyroplastics, plasticrusts or anthropoquinas), Domínguez-Hernández et al. (2022), suggested to consider the finding unprecedented and the agglomerate unique, thus deserving a specific classification. Under this view, they named this formation "plastitar" in addition to emphasizing the need for further studies to underline the occurrence of this pollution in other regions of the world, to measure its extent worldwide, and to highlight the potential negative impacts for the marine environment.

Following this indication and aiming also to add further knowledge about the chemical composition and the processes leading to plastitar formation, we searched for the occurrence of similar formations in the Mediterranean Sea and found them to be widespread along the Mediterranean rocky shorelines. We report data from four different geographical areas that were therefore surveyed by collecting replicated samples: the Ligurian coast (North Mediterranean Sea, Italy), the Salento coast (Southern Adriatic Sea, Italy), Sardinia (South West Mediterranean Sea, Italy,) and the Balearic Islands (Western Mediterranean Sea, Spain). For each sample, we performed visual and chemical characterization of both the micro- and meso-plastics admixed to the tar residue. The tar was fingerprinted in an attempt to trace-back their seep origin by using bulk geochemical biomarkers, recognized by means of gas chromatography coupled to mass spectrometry (GC–MS). Specifically, we considered the distribution of n-alkanes (from light-medium weight to high-weight), aromatics, isoprenoids and the parameter ratios of refractory terpanes and steranes for tracing genetic similarities according to established literature methods (Hostettler et al., 2004).

2. Material and methods

2.1. Study area and sample collection

A total of 19 plastitar residues from 11 different coastal locations were collected over a five years' time span (April 2018–December 2022), in areas patrolled by both scientists and citizen scientists recruited through a dedicated social media campaign. Fig. 1 shows the location of all sampling stations where plastitar samples were found and collected. The detailed list of all samples is provided in Table 1 together with a brief description of the sampling locations and of the formation as it was visualized on the day of sampling, the geographical coordinates, the sampling date and the number of samples collected. Additional information about the sampling locations is provided in the Supplementary material together with extensive photographic documentation of all plastitar samples collected (Supplementary Section 1). To estimate plastitar coverage onto rock surfaces in selected sampling locations, five different sampling areas, at least three meters apart from each other were selected, covering a total of 15–50 m^2. At each location, four different quadrants of 20 × 20 cm were randomly selected for the sample collection, thus following a sampling approach similar to that described by Domínguez-Hernández et al. (2022). All the material inside the quadrant was removed from the rock with the help of a hammer and metal scalpel, then wrapped in aluminum foil and placed in pre-cleaned glass jars for transport to the laboratory where the chemical and morphological analysis were performed. Approximately 50 g of material was retrieved from each sampling location, with variation depending on rock surface coverage and tar mat thickness. The same day of the

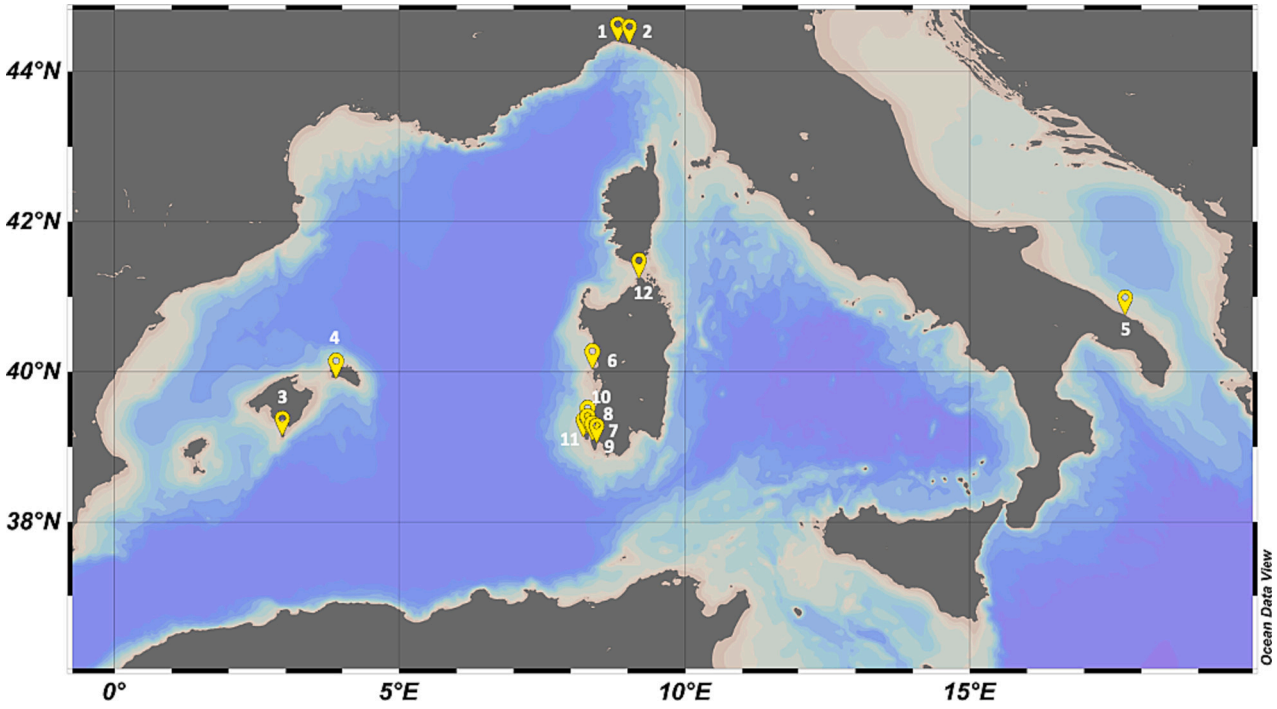

Fig. 1. Map of the central-western Mediterranean Sea showing the locations of all plastitar samples collected during this study. For more details on the sampling locations the reader is referred to Table 1 and to the Supplementary material.

Table 1
Description, name, date, region, GPS coordinates and coastaline orientation of all plastitar sampling locations described in this study. Indication about the total area surveyed (in square meters), the rock surface coverage (%), and of the sample appearance on the day of sampling are also provided.

Station number	Location name	Sea pertinency	Coordinates	Coastline orientation	Total area surveyed (mq)	Sample I. D.	Sampling date	Description of the formation
1	Sturla	Ligurian Sea	44°23′29.4″N 8°59′10.3″E	S	15	*ST*	12/9/2022	Fresh tar splotch
2	Bogliasco, Pontetto	Ligurian Sea	44°22′31.5″N 9°04′34.8″E	S-SE	n/d	*BO*	15/8/2022	Asphaltite appearance
3	Cabrera National Park	Balearic Islands	39°08′38.285″N 2°56′12.217″E	N-NW	n/d	*BA1*	31/7/2019	
4	Menorca Island	Balearic Islands	39°55′32.225″N 3°53′52.195″E	S-SW	n/d	*BA2*	13/11/2022	Waxy bitumen appearance
5	Specchiola Carovingo	Adriatic Sea	40°43′49.6″N 17°45′19.7″E	NE	25	*P1*	06/07/2022	Weathered tar appearance
6	Capo Mannu	Sardinia	40°03′04.3″N 8°24′05.6″E	N - NW	20	*OR1* *OR2*	6/8/2022 6/8/2022	Tar appearance
7	Cala Sapone	Sardinia	39°00′25.8″N 8°23′04.5″E	W-SW	n/d	*SA*	14/11/2022	Tar appearance
8	Calavinagra	Sardinia	39°09′50.0″N 8°14′30.2″E	N - NW	25	*CV*	20/12/2022	Massive weathered tar mat on a rocky inlet, strong petroleum odorous
9	Cala di Memmerosso	Sardinia	39°10′41.5″N 8°16′49.6″E	N - NW	15	*CF1* *CF2* *CF3* *CF4* *CF5* *CF6* *CF7* *CF8*	12/04/2018 20/10/2020 7/02/2021 17/9/2021 20/12/2021 29/4/2022 4/10/2022 19/12/2022	Massive weathered tar with a waxy bitumen appearance, on a rocky inlet
10	Capo Spalmatore	Sardinia	39°07′00.1″N 8°15′27.8″E	W - NW	15	*LC*	16/12/2022	weathered tar ball on a sandy beach
11	Capo Sandalo	Sardinia	39°08′40.7″N 8°13′20.6″E	W - NW	15	*CS*	23/12/2022	tar with asphaltite appearance on a rock, strong petroleum odorous
12	Capo Testa	Bonifacio Strait	41°14′15.7″N 9°08′30.1″E	W-SW	n/d	CT	14/8/2022	Not sampled. Only photographic record available

plastitar collection, a brief description of the larger debris observed in the sample location during the operation was also compiled. Once in the laboratory, all plastitar samples were photographed, weighed, and divided into two aliquots. One aliquot of 2 g was submitted to SARA and GC–MS analysis while the remaining material was submitted to plastic particle identification and characterization.

2.2. Microplastic analysis

For determining MPs concentration, "plastitar" samples were carefully scrutinized layer by layer starting from the top (the outer layer exposed to the open air) and reaching the bottom (the layer in contact with the rock surface). For ease, we considered three distinct sections: top, inner and bottom. To avoid external contamination, sample manipulation was carried in a dedicated fume hood and employing stainless-steel tweezers. All suspected plastic particles identified by the naked eye were isolated and submitted to FTIR analysis. The size, shape and color of the items positively identified as synthetic polymers was then reported. Any other material apart from plastic found in the tar matrix was also described. Particles displaying sizes between 1 and 5 mm were classified as large MPs, while larger items were counted as meso/macro plastics (> 5 mm). Considering the shapes, both MPs and meso/macro plastics were classified as foams, films, nurdles, fibers, lines and fragments according to literature indication (Crawford and Quinn, 2017). For color classification we followed the indications provided by Martí et al. (2020). An attempt to isolate smaller MPs (< 1 mm) were carried out by dissolving 5 g of tar for each sample in 20 ml of toluene and by filtering the resulting mixture onto stainless steel filters (paco filter, 20 μm mesh size) using a vacuum apparatus. The synthetic identity of the particles extracted from the plastitar samples was confirmed through ATR-FTIR spectroscopy performed using a Nicolet IS10 ATR/FTIR spectrometer (Thermo-Fisher Scientific) for the analysis of large MPs (1–5 mm) and a Spotlight 200i FT-IR (Perkin Elmer Italia S.p.a., Milano, Italy) for the recognition of small MPs (<1 mm) onto the stainless filter. Prior to FTIR analysis, the particles were washed with cyclohexane in an ultrasonic bath Sonica S3 (Soltec s.p.a, Milano, Italy) for 10 min to remove residual tar from the surface and to enable a correct identification of the constituent polymers. Analyses were carried out following a point mode acquisition procedure previously described (Saliu et al., 2023). IR spectra were recorded by using the diamond attenuated total reflectance (ATR) unit and a liquid nitrogen cooled mercury cadmium telluride (MCT) single detector, applying a wavenumber range 4000–400 cm^{-1}, resolution of 4 cm^{-1} and 32 co-added scans. Patented COMPARE™ spectral comparison algorithm (by Perkin Elmer) was used to confirm the synthetic origin of the particles as previously reported (Saliu et al., 2018). The minimum matching for positive identification was set at 70% as indicated in the Guidance of Marine Litter in European Seas of the European Commission (Galgani et al., 2013).

2.3. Morphological description of the tar residues

For a first visual categorization of the tar residues, we applied the class distinction proposed by Corrick et al. (2021). Briefly, this categorization system is based on the recognition of key morphological features that may be assessed by the naked eye. It includes the classes asphaltites, waxy bitumens and tars. Asphaltites appear usually as solid and brittle aggregates that easily break apart with a characteristic conchoidal fracture and display deep shrinkage cracks across their outer surface and no presence of sediments in the internal layers. Waxy

bitumens are recognized by their black dull color and their slight greasy luster. They cannot be considered entirely brittle since they present an externally brittle layer and a pliable interior. Tars appear as sticky and viscous deposits, characterized by the ease of deformation and the absence of rigid structure. The malleability can be considered their key distinctive features, since differently from asphaltites and waxy bitumen, they are easily deformed even under a mild pressure.

2.4. Chemical characterization of the tar residues

Tar was chemically characterized according to the standard analytical method ASTM D6560 (standard test method for determination of asphaltenes in crude petroleum and petroleum products) and of the ASTM D4124–9 (Standard Test Method for Separation of Asphalt into Four Fractions) for the determination of saturates, aromatics, resins, and asphaltenes (SARA) with slight variation. Briefly, 1.0 g of tar residue were diluted in a 15 ml round bottom flask containing 8 ml of n-heptane, stirred for 30 min at 1500 rpm and then left to settle for 2 h to induce asphaltene precipitation. After that the mixture was filtered onto quartz fiber filters (Whatmann QMA, 47 mm, 2.2 um) and the asphaltene content was determined by measuring the weight of the precipitate collected by filtration. The filtrate (maltene fraction) was dried using a rotavapor apparatus (Buchi Labortechnick, Postfach, Switzerland) and the residue was weighed for mass balance confirmation. A 1.5 g aliquot of the residue was then diluted in 20 ml of hexane and placed on top of a chromatographic column containing silica gel for flash chromatography (230–400 mesh). The chromatographic separation of the SARA fractions was obtained by eluting with 100 ml hexane (isolation of saturates); 100 ml of toluene (isolation of aromatics); 100 ml of toluene-methanol solution (50:50) (isolation of polar compounds and resins); 100 ml of methanol-chloroform solution (50:50) (elution of residual polar compound and resins). Each fraction was then dried under vacuum by using a rotavapor Buchi R-300 (Buchi, Labortechnik, Postfach, Switzerland), and stripped with nitrogen to remove the residual solvent. The residues were finally weighed with an analytical balance (Gibertini, Milano, Italy) to assess the relative recovery of each fraction. For data reporting, the saturate, aromatic and resin contents were expressed as weight percent of the residue compared to the total tar weight. In addition, tar density was evaluated by pycnometer measurements according to ASTM D70–03, and the elemental profile was investigated by using a CHN/S analyzer 2400 Series II CHNS/O from Perkin Elmer (Perkin Elmer Italia S.p.a, Milano, Italy).

2.5. GC–MS analysis on tar residues

For the identification of petroleum geochemical markers 100 mg of tar samples were dissolved in 5 ml of hexane by 15 min sonication and filtered through glass wool to remove particulates. The solution was then submitted to silica gel flash chromatography for a preliminary compound class separation. A 25 cm diameter glass column was filled with 8.5 g of silica gel (Mesh 70–230 sigma Aldrich-Merck). The top of the column was covered with a layer of activated copper and deactivated neutral alumina (approximately 3 mm in total). Two fractions were then collected by gradient elution, specifically the first eluate was obtained with 200 ml of hexane to collect the saturated alkanes, a second fraction was eluted with hexane: dichloromethane 70:30 to collect aromatic compounds. Both these fractions were then evaporated to dryness and diluted approximately to 100 ppm concentration level in dichloromethane for the subsequent gas chromatography - mass Spectrometry (GC/MS) analysis that was carried out by employing an Agilent 7920 A-5977B instrument (Agilent Technologies, Santa Clara, US). 1 μl of the isolated residues was injected and the chromatographic system at 280 °C and in split mode with a 20:1 split ratio. The analytes were separated by using a DB-5MS capillary column 60 m × 0.25 mm with film thickness 0.25 μm (Agilent Technologies, Santa Clara, USA) and by applying a column gas flow of 1.0 ml/min of He used as carrier gas. The following temperature program was applied: 5 min at 40 °C, 7 °C/min to 310 °C than 310 °C for 20 min. Mass spectrometer was operated in full scan mode from 40 to 500 amu (Scan Speed: 781u/s; Scan Frequency: 1.7; Cycle Time: 600 ms).

The identification of the chemical species was performed by comparison with available standards (when available) and/or by using a mass spectra library (NIST 20), and/or by comparison with published reference spectra for a tentative identification. Kovat retention time index (Kovats, 1958) was used as confirmation criteria for the positive identification. Each or summed area of the identified compounds were then used to determine the geochemical parameter ratios, and the obtained values were used to tentatively group the samples. The geochemical indicators were selected from the literature to include as many as possible of the chemical families and constituents that previous literature works indicate as being common in the tar and with a seep tracing capability.

Specifically, the main petroleum related analytes and the specific geochemical markers researched for tar source identification were:

- Occurrence and distribution of n-alkanes (C5–C40 carbon range) that are known to strictly depend on the sources of carbon from which the petroleum is generated, the geologic environment in which they migrated and the reservoir, the refining process (when the spill is related to an anthropogenic source), and the extent of the weathering process after the spill (Wang et al., 2006).
- Occurrence of volatiles hydrocarbons including BTEX (benzene, toluene, ethylbenzene, and three xylene isomers) commonly used to highlight possible recent spills and their relative amounts compared to paraffins and naphthenes (mainly cyclopentane and cyclohexane compounds) (Wang and Fingas, 2003).
- Relative amounts of paraffinic, naphthenes, aromatic, resin, and asphaltenic compounds.
- The occurrence of EPA priority PAHs and of their petroleum-specific alkylated (C1–C4) homologues (i.e., alkylated naphthalene, phenanthrene, dibenzothiophene, fluorene, and chrysene) that provide valuable insight regarding the chemical makeup of the oil.
- The occurrence of alkylated aromatic heterocycles (N, O, S). These compounds are generally present in fresh crude oils at quite relatively low concentrations compared to PAHs and become enhanced with weathering because they are biorefractory and persistent in the environment.
- The pristane to phytane ratio, commonly indicated as Pr/Ph index and used both to estimate the degree of oil bio-degradation in the environment and to compare oil source (Peters and Moldowan, 1993; Wang et al., 2006; Christensen and Larsen, 1993).
- The ratio between the geochemical markers 17a-22,29,30-trisnorhopane and 18a-22,29,30- trisnorneohopane (Tm/Ts index), that is commonly used as both a source and maturity parameter (Seifert and Moldowan, 1978).
- The “Triplet” index, a source parameter used to distinguish coastal tar residues in (Kvenvolden et al., 2000). This index is calculated by considering the relative area of C26 tricyclic terpanes, R and S stereoisomers (extracted with mass *m/z* 191 and identified by occurrence of the molecular ion at m/z = 360), and the area of C24 tetracyclic terpanes (extracted mass m/z 191 and molecular ion m/z = 330.3). A characteristic value of the index (triplet >3) is attributed to anoxic environments.
- The ratio between the C23 tricyclic terpane and the C24 tricyclic terpane (23Tri/24Tri) also used as source parameter (Page et al., 1999)
- The C31S/(S + R) maturity parameter this ratio is based on the occurrence of hopane epimers and it is commonly used as maturity parameter in petroleum geochemistry; the equilibrium ratio at full mature petroleum is established at 0.6 (Ensminger et al., 1974; Mackenzie, 1984).

- The "23 T/C30" ratio, calculated by considering the molecules C23 tricyclic terpane and 17a,21b(H)-hopane and commonly used as a source parameter (Peters and Moldowan, 1993).
- The 17a,21b(H)-hopane/17a,21b(H)-30-norhopane ratio (C30/C29) firstly introduced by (Palacas et al., 1984) and then widely used a source parameter.
- The bisnorhopane Index (BI) based on the ratio between 28,30-bisnorhopane and 17a,21b(H)-hopane. This index is used to identify oils sourced from near-surface facies. The presence of high 28,30-bisnorhopane (high BI index) is in general related to anoxic highly-reducing depositional marine environments (Curiale et al., 1985). Moreover, BI was found to decrease with thermal maturity (Peters and Moldowan, 1993).
- The oleanane index (OI) obtained by considering the ratio between 18a + b(H)-oleanane/17a,21b(H)-hopane and commonly used as source parameter to indicate a contribution from Cretaceous and younger plant material (Peters and Moldowan, 1993).
- The gammacerane index (GI), obtained considering the ratio between gammacerane/and 17a,21b(H)-hopane and used as a source parameter because abundant gammacerane was found to be related to carbonate/evaporite facies and marker for highly reducing, hypersaline depositional environments (Peters and Moldowan, 1993).
- The diasteranes/sterane index, that is related to thermal maturity, lithology and redox potential of the depositional environment. Steranes are extracted at $m/z = 217$ while diasteranes m/z = 259. Steranes are known to be converted into diasteranes by acid catalysis. Diasteranes when formed are more stable then steranes (therefore the index trace oils from mature to early postmature). Very low level of diasteranes in comparison to regular steranes commonly indicates also clastic-poor marine source rock.
- The Perylene/Chrysene ratio is an indicator based on the relative abundance of these two PAH compounds. Perylene is commonly used to distinguish shallow-seeping oils from deeper oils since it displays a biogenic origin and it is associated with near-surface bitumens (Venkatesan, 1988).
- The Polycyclic Aromatic Hydrocarbon - Refractory Index (PAH-RI) an index commonly used as a source parameter. Abundance of aromatized steranes, especially monoaromatics relative to triaromatics, indicates low thermal maturity of petroleum (Curiale et al., 1985). Thus, the indicator is obtained by considering the peak at m/z 231 that is usually the second major peak in in the highly refractory triaromatic sterane (C26 to C28) and the peak at m/z 242 to that of the first, usually dominant, peak in the monomethyl chrysenes (Hostettler et al., 1999).
- The aromatic steroid parameter T/(T + M) used as thermal maturity and source parameter (Peters and Moldowan, 1993). Low values of this index are reflecting relatively high levels of the monoaromatic steroids and indicate low thermal maturity. For calculation T corresponds to the triaromatic steranes total areas (from C26 to C28) extracted at m/z 231, while M indicates the total monoaromatic steranes areas (also in this case from C26 to C28) extracted at m/z 253.
- The dimethyl dibenzothiophenes/dimethyl phenanthrenes index ($\sum$C2D/$\sum$C2P) commonly used as a source parameter (Kaplan et al., 1997; Bence et al., 1996) This index is based on the comparison of the levels of sulfur-containing PAH to the levels of regular PAH and obtained by considering the ratio between the extracted ion current related to m/z 212 and to m/z 206, respectively.
- The $\sum$C3D/$\sum$C3P index, used similarly to the $\sum$C2D/$\sum$C2P index and obtained by considering the ratio between trimethyl dibenzothiophenes (at m/z 226) and trimethyl phenanthrenes (at m/z 220).

2.6. Solvents and reagents

Analytical grade solvents (Hexane, Heptane, Dichloromethane, Methanol) were purchased from Sigma Aldrich (Merck KGaA, Darmstadt, Germany). Naphtalene-d_8 and C7-C40 saturated alkanes standard also from Supelco (Merck KGaA, Darmstadt, Germany) were used as reference standard to calculate recoveries and evaluate Kovats retention index. Nitrogen (99,9995 % purity) and Helium bip grade were provided by Sapio (Sapio Industria S.p.a., Monza, Italy).

2.7. Statistical analysis

The collected data were submitted to multivariate statistical analyses to sort out the differences in the biomarker ratios, to test for correlations between and within the sample groups, and to attempt to group the collected samples according to possible common sources. Analyses were performed by employing the XLSTAT data analysis software package (Lumivero, Denver, US). The Mann-Whitney test was used to evaluate significant differences in microplastic distribution among the different samples, also by considering the different microplastic features (classification by size, shape, color, polymers). The principal component analysis (PCA) tool was applied to reduce the dimensionality of the dataset, highlight relationships among variables and to assess the contribution of each variable to the overall variance of the data. Prior to the PCA analysis, the data was first standardized by the variable mean and standard deviation.

3. Results

3.1. Plastic particles counts and characterization

A total of 801 suspected plastic particles were extracted from the 19 plastitar samples object of this study and confirmed as microplastics by Fourier transform infrared (FTIR) spectroscopy. More specifically 377 (47.1 %) were found in the size range 1–5 mm and catalogued as microplastics, 424 (52.9 %) resulted larger than 5 mm and were considered as *meso*/macroplastics. Some examples of the particles extracted are shown in Fig. 2.

Considering colors, 67.7 % of the particles were yellow, 19.5 % were brown, 6.7 % white/transparent, and all the remaining colors (blue, red, grey, black, and green) accounted for <5.0 % in total (Fig. 3A). Considering the constituents polymers, polyolefins resulted the most commonly detected both in the micro and meso/macroplastic fraction (Fig. 3B). Specifically, PE and PP accounted for 74.9 % and 21.2 % of the detected particles respectively. Other detected polymers were PVC (1.0 %), PA (0.9 %), PVC (0.7) and PS (0.5 %). Considering shapes, 34.1 % of the items were classified as fragments, 32.2 % as nurdles, 20.5 % were lines, 13.0 % were films, <1.0 % were foam (Fig. 4A). In the microplastic size range (items <5.0 mm) nurdles resulted the most abundant with 87.2 %, fragments were 6.0 % and film were 5.2 % (Fig. 4B). Table 2 reports the details regarding the particle concentrations determined in the different plastitar samples. The maximum concentration was found in sample CF5 (Cala di Memmerosso, Sardinia) and was equal to 2.1 items/g. The highest relative concentration of MPs was found in sample BA2 (Menorca Island, Spain) with 81.8 % of the detected plastic items <5.0 mm; while the lowest was found in sample ST (Sturla, Ligurian Sea).

Fig. 5 reports the comparison of the number of particles found at inner and outer surfaces for each particle shape, as well as considering the whole dataset. In terms of absolute counts, the number of particles detected on the outer surfaces and in the inner core of the tar mat resulted comparable with the total number of detected plastic items (451 and 328, respectively). Considering particles shapes, the plastitar surface (the external layer exposed to the open air) mostly incorporated fragments and nurdles (Fig. 5), while the inner core showed a prevalence of lines and films. The number of particles found in the bottom layer of the tar mat (the surface attached to the rock) was negligible in all cases.

Statistical analysis carried out by considering data grouped according to sampling location (sea pertinency) did not highlight any significant difference in terms of total plastic concentrations (Kruskall Wallis,

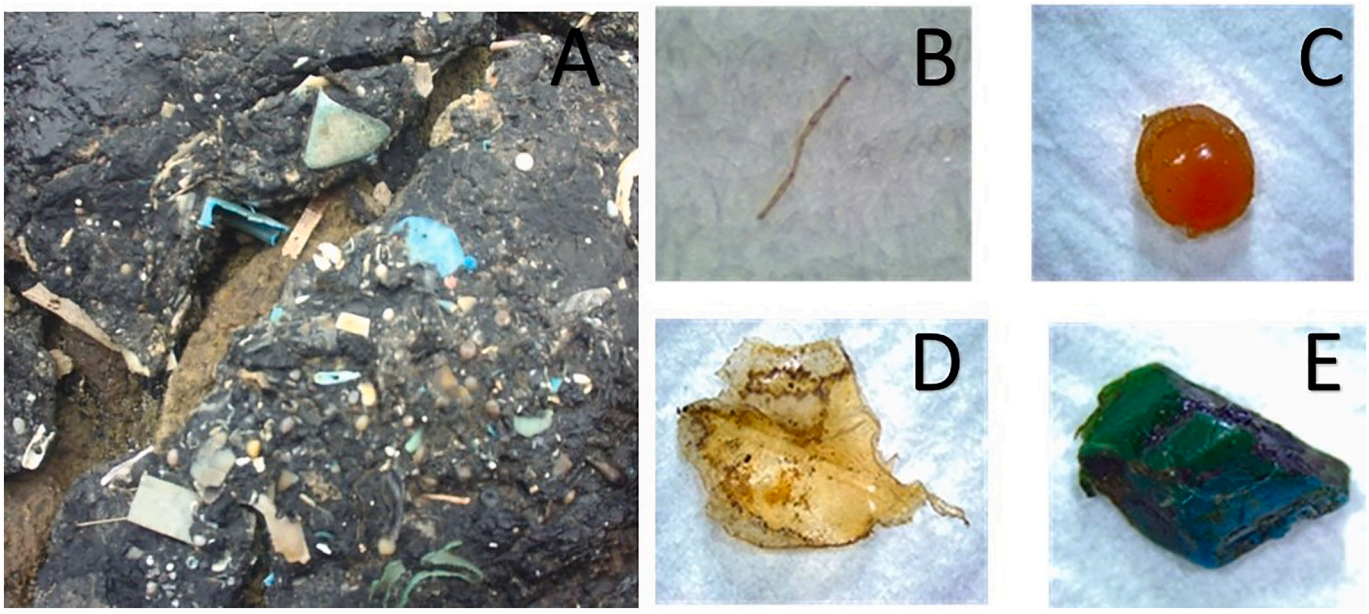

Fig. 2. examples of plastitar (A) found in the Mediterranean Sea costal areas and of the plastic particles typologies extracted from their inner and outer layers. B: line; C: nurdle; D: E: fragment.

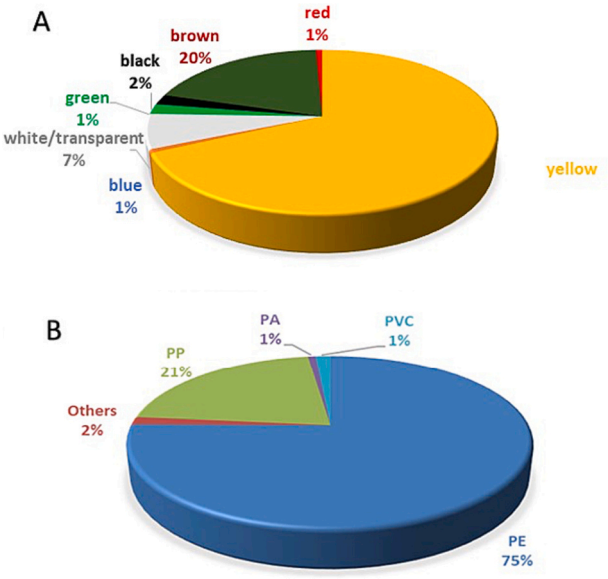

Fig. 3. Colors (A) and polymers (B) of the plastic particles extracted from Mediterranean plastitar samples. PA = Polyamide; PVC = polyvinylchloride; PE = polyethylene; PP = polypropylene.

$p = 0.971$, alpha = 0.050). Significant differences were instead observed by considering particle shapes (Kruskall Wallis, $p = 0.874$). More specifically, considering both micro and meso-plastics, fragments resulted to be significantly more abundant than film and lines (Mann Whitney, $p = 0.003$ and $p = 0.005$ respectively), while considering microplastics, nurdles resulted significantly higher than fragments, films and lines (Mann Whitney, $p = 0.012$, $p = 0.004$ and $p = 0.009$ respectively). Considering the particle's distribution between the inner and the outer plastitar layers (normalized for the total mass of the sample), pellets and fragments displayed significantly higher concentration in the outer layers if compared to the inner layers (Mann Whitney, $p = 0.014$ and $p = 0.002$ respectively). More details of the statistical analysis are reported in the supplementary section associated to this article (Supplementary section S3).

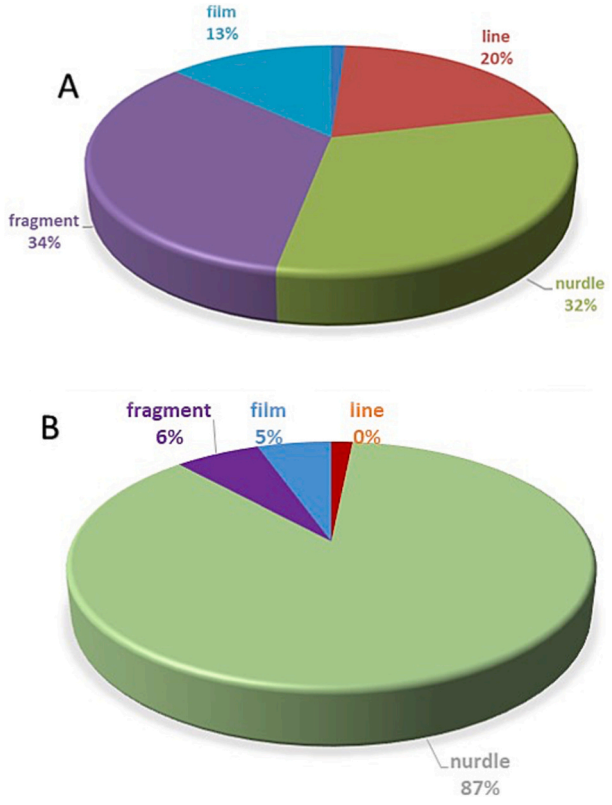

Fig. 4. Particle shape distribution observed in all plastic items extracted from Mediterranean plastitar samples (A) and only in the microplastic particles (B).

3.2. Tar characterization

Table 1 reports a categorization of the tar fraction of the collected plastitar samples, obtained by considering qualitatively their key morphological features. Seven samples displayed a semi-solid consistency with the presence of a pliable inner core (OR1, OR2, CV, CF1, CF2, CF3, CF4) and were categorized as waxy bitumen. Three samples (BO,

Table 2
Concentration of plastic fragments, fiber films and pellets extracted from the different plastitar samples and percentage of the microplastic fraction (i.e., particles <5 mm). Values are all expressed as items/g.

Sample ID	Fragments	Films	Pellets	Lines	Total	Micro %
ST	0.11	0.22	0.43	0.38	1.14	38.1
BO	n.p.	n.p.	n.p.	n.p.	n.p.	n.p.
BA1	0,04	0,06	0,20	0,07	0,36	61,0
BA2	0,33	0,08	0,5	0,00	0.91	81.8
OR1	0,04	0,03	0,23	0,03	0,32	75,0
OR2	0,06	0,02	0,14	0,02	0,23	60,0
CF1	0,19	0,17	0,21	0,40	0,98	32,6
CF2	0,16	0,16	0,43	0,14	0,89	53,8
CF3	0,12	0,02	0,09	0,02	0,26	81,6
CF4	0,04	0,11	0,15	0,11	0,41	36,8
CF5	0,19	0,47	0,94	0,41	2.00	50,0
CF6	0,26	0,10	0,51	0,51	1,38	44,2
CF7	0,03	0,03	0,10	0,03	0,20	50,0
CF8	0,00	0,05	0,26	0,21	0,52	59,8
CV	0,55	0,02	0,14	0,07	0,78	32,7
P1	0,29	0,01	0,26	0,08	0,63	54,0
SA	n.p.	n.p.	n.p.	n.p.	0.09	100
LC	0.012	0.02	0.12	n.p.	0.15	100
CS	n.p.	n.p.	n.p.	n.p.	n.p.	n.p.
Mean	*0.148*	*0,104*	*0.293*	*0.177*	*0.344*	*0.378*
S.D.	*0.146*	*0.124*	*0.227*	*0.174*	*0.236*	*0.306*

LC, SA) displayed a more solid consistency and embrittlement, with presence of conchoidal fracturing, and were categorized as asphaltites. The rest of the samples displayed the classical appearance of weathered tar, and therefore were classified as tar. Marked differences were also observed by considering the sticky feel on hands, since some samples resulted more prone to leave a grease difficult to remove when touched (CF6, P1, ST, CS) while other samples displayed a rocky consistency and no signs of sticky behavior (LC, SA). Regarding the petroleum odorous some samples displayed a very strong petroleum odorous (CV, P1) while others produced a less intense odor (CS, OR2).

Details of the chemical characterization of the collected samples are provided in Table 3. Density measurements showed an average of 1.15 g/cm^3 (SE 0.18) with a maximum value of 1.51 found in sample LC and a minimum value of 0.93 found in sample OR1. SARA analysis revealed that the materials were mainly composed of high molecular components with asphaltenes and resins covering the 27–42 % and 14–51 % of the total tar mass, respectively. Appreciable amounts of saturated hydrocarbon (2–5 %) and aromatics (3–7 %) were also detected. CHN/S measurements showed variation in the sulfur content from 1.3 to 4.3 % and of nitrogen from 0.3 to 1.27 % (Supplementary section S2). Carbon-hydrogen ratio resulted varying from 6.1 to 17.2 with an average of 8.1.

GC–MS analysis displayed a variety of chemical compounds that were fingerprinted by selective research of the most significant ion related to the structural backbones of each molecular class as detailed in the experimental section. The complete list of the GC–MS profiles resulting from the plastitar analysis is reported in the supplementary file (Supplementary, sections S2 and S4). Fig. S4.1 reports an overview of the main chemical structures identified. In fig. S4.2 a typical total ionic current (TIC) profile collected operating in full scan analysis mode is depicted, from which the extracted ion chromatograms (EIC) of isoprenoids (*m/z* 57), beta-carotenoids EIC (m/z = 125), terpanes/hopane

Table 3
Results of the SARA analysis.

Sample ID	Density (g/cm^3)	Saturates (%)	Aromatic (%)	Asphaltenes (%)	Resins (%)
ST	0.98	1.7	5.7	49.1	39.7
OR1	0.93	3.5	7.9	48,6	37.9
OR2	0.99	3.7	8,9	45.8	39.8
CF1	1.04	1.3	5.2	50.8	41.7
CF2	1.31	1.1	4.9	48,5	40.2
CF3	1.11	6.7	5.0	45.8	39.5
CF4	1.16	3.4	5,9	53.8	33.1
CF5	1.30	3.7	4.0	48.6	38.2
CF6	1.00	1.2	6.9	44,2	40.1
CF7	1.30	2.6	4.8	47,2	39.1
Cf8	1.12	1.0	6.4	48,4	37.9
CV	1.23	1.3	3.6	45,8	39.6
P1	1.09	6.7	11.3	48.1	33.9
BA 1	1,13	1,2	5,9	50.7	39.8
BA 2	1,08	0,9	4,9	50.8	41.7
SA	1,30	1.0	5.0	48,6	37.9
BO	1.46	1.4	9,1	42.0	47.2
LC	1.51	0.7	4.0	36,9	61.3
CS	1.23	1.7	4.9	28.7	65,1
Mean	*1.15*	*2.8*	*6.7*	*46.5*	*41.7*
SE	*0.18*	*1.9*	*2.0*	*5.7*	*8.1*

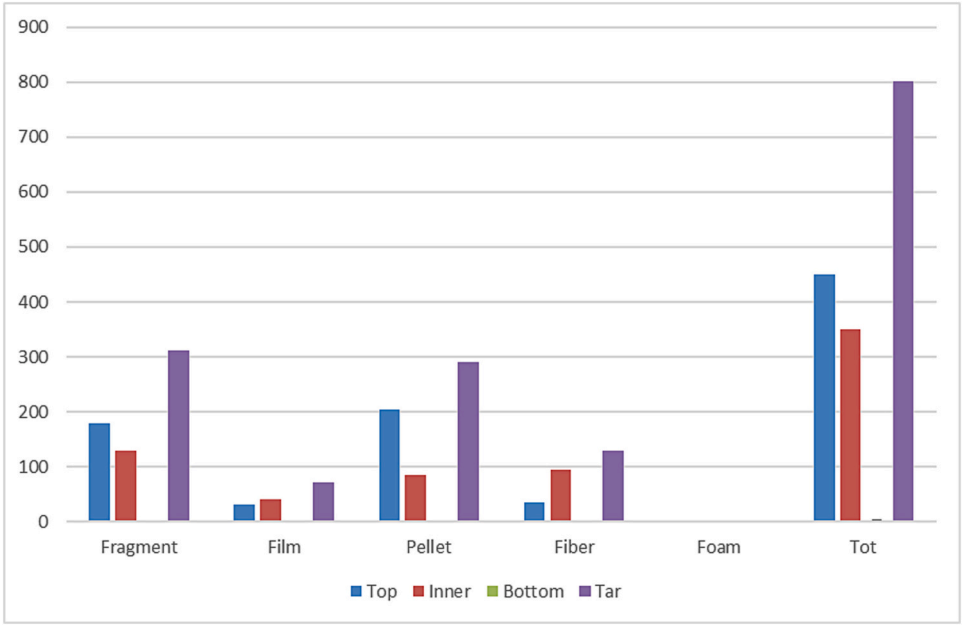

Fig. 5. Relative frequency distribution of fragments, films, lines, pellets and foam extracted.

(m/z = 191), steranes (m/z = 217), triaromatic steranes (m/z = 231), diasteranes (m/z = 259), monoaromatic steroids (m/z = 253), monomethyl chrysenes (m/z = 242), dimethyldibenzothiophenes (m/z = 212), trimethyldibenzothiophenes (m/z = 226) and dimethylphenanthrenes (m/z = 220) were extracted. Fig. S4–3, S4–5, and S4–6 are representative of the resulting extracted ion chromatogram obtained and of the identified targeted compounds. Overall linear n-saturated alkanes, cyclic alkane, aromatic hopanes and steranes were found in all the samples. None of the samples displayed the typical unresolved profile of hydrocarbons that in the literature is commonly named as unresolved complex mixture (Curiale et al., 1985). Moreover, no short chain alkanes and BTEX were detected. The occurrence of intact isoprenoids (n-C17/pristane and n-C18/phytane) was highlighted only in samples BA1, BA2 and CS with values of the Pr/Ph ratio varying from 0.1 to 0.5. Medium-long chain n-alkanes (C < 15) showed a large variety of profiles (Supplementary S2.5), with distribution ranging from paraffinic to aromatic asphaltic. In more details, samples LC, CV and BO resulted in a monomodal distribution characterized by relatively low C35-C39 *n*-alkane response. Samples CS and SA displayed a bimodal distribution with still low C35-C39 *n*-alkane response. Samples CF1, BA1, BA2 and P1 displayed a bimodal distribution with relatively higher C35-C39 *n*-alkanes, grading thus into solid waxes. Samples CF2 and CF3 displayed a very unusual trimodal distribution. The peak areas of the selected geochemical markers were retrieved from the extracted chromatograms and integrated to calculate the geochemical parameters as detailed in the experimental section. The obtained values are listed in Table 4. Since the highly degradation-resistant (C30)17a(H), 21b(H)-hopane was found in all the samples it was selected to serve as conserved "internal standards" for determining the extent of weathering in relationship to other detected biomarker (Wang and Fingas, 2003). Overall, steranes (tricyciclic and pentacyclic) occurred in all the samples but resulted relatively low in comparison to hopane, thus indicating that most tar residues originated from oils that reached full maturity. The hopane maturity index [C31S/(S + R)] showed values between 1.04 and 1.42 that indicates high maturity of the tar residue (Ensminger et al., 1974; Mackenzie, 1984). However, the thermal maturity index based on the occurrence of aromatized steranes (T/T + M) resulted in varying from 0.12 to 0.87 thus highlighting a certain variability in the thermal maturity was retrieved. This variability was confirmed also by the absence of diasteranes, that were detected only in sample BO, and the variable amounts of perylene/chrisene index (ranging from 01 to 4.6) that is commonly linked to deep. Also, Bisnorhphane ratio (BI) (that is also related to deep) resulted to vary from 0.231 to 0.453 with the lowest values found in samples ST, BO and CS. Indicators of anoxic marine depositional environment, such as 28,30-bisnorhopane (Curiale et al., 1985), gammacerane and high values of C35 ab-hopane 22S and 22R epimers compared to C34 (Peters and Moldowan, 1993) were highlighted in samples BA1, OR, P1 and PS but with discrepancies (anoxic environment was not confirmed by all the indexes). Alkylated PAH compounds (chrysenes) and sulfur-containing PAH, such as dibenzothiophene that are known to be the most degradation resistant among aromatic hydrocarbons (Wang and Fingas, 2003) were found in all the samples. The related ∑C2D/∑C2P and ∑C3D/∑C3P that express ratio between sulfur containing and regular PAH were found to vary from 0.3 to 4.0. These values are similar to those reported from previous literature studies but again from various locations. The refractive index (RI) was found to vary from 0.5 to 5. Literature reports for instance values varying from 10 to 80 (Wang). Finally, the relative ratios of paired terpane compounds that are known to not be altered by weathering including Ts = Tm, C23/C24, C29/C30, C31 22S/(22S + 22R), C32 22S/(22S + 22R), C33 22S/(22S + 22R), also showed high variation in the sample set.

3.3. PCA results

The result of the PCA carried out on the dataset including the geochemical indicators is reported in Fig. 6. As depicted, the loadings plot is showing a marked differentiation of sample BO along PC1. In this principal component the highest contribution is provided by the Per/Chry index (14.7 %) and the C31S/(S + R) index (12.3 %). Correlation matrix (Supplementary material S3) highlights a significant correlation between T/(T + M) and C31S/(S + R), between T/(T + M) and the triplet and Pr/Ph, and also between PAH-RI and GI. Since all these parameters are indicator both of thermal stability and indicator of source (oxic or anoxic environment), their correlation must be considered a direct consequence of the grouping of the tar samples according to their different seep origin, operated by the principal component analysis. Along PC2, sample ST is scoring the highest positive values and results are markedly differentiated from sample CF2. Along this principal component the major contribution is related to C30/C29 (22.5 %) and ∑C2D/∑C2P (27.5 %).

The results of the PCA performed including plastic concentration and geochemical indicators is reported in the Supplementary (Section S3). Also, in this case sample BO and ST results differentiated as outliers and also sample CF1 and CF2 built a distinct cluster. The correlation matrix highlighted some interesting correlations between lines concentration, film concentration and BI, C30/C29 geochemical indicators, as a consequence of the different distribution of plastics in the different tars from different locations displaying a different seep origin.

4. Discussion

4.1. Distribution of plastic in the layered structure of the plastic tar

We extracted a total of 801 plastic particles from 19 plastitar samples (total weight 1370 g), yielding an average concentration of 580 plastic items/kg of plastitar. In the study carried out by Domínguez-Hernández et al. (2022), no concentration data was provided, so this must be considered the first information regarding plastic concentrations in plastitar. In terms of absolute concentrations, this value is comparable to

Table 4
Identification of the main biomarkers found in the Mediterranean plastitar samples (n.p. the marker was not detected).

Sample ID	Pr/Ph	Tm/Ts	triplet	C31S/(S + R)	C30/C29	BI	GI	PAH-RI	T/(T + M)	∑C2D/∑C2P	∑C3D/∑C3P	Pery/Chr
BA1	0.214	1.392	0.220	1.234	0.452	0.376	n.p.	1.604	0.614	2.038	2.682	0.139
BA2	0.156	1.069	0.269	1.330	0.729	0.238	n.p.	1.622	0.476	1.548	2.595	0.247
CF1	n.p.	1.214	0,197	1.253	n.p.	0.028	n.p.	0.654	0.654	1.670	2.315	0.117
CF2	n.p.	1.089	0,216	1.286	0.924	0.273	n.p.	2.679	0.419	2.408	3.363	4.178
CF3	n.p.	1.32	0,206	1.285	0.734	0.255	n.p.	2.168	0.534	1.641	0.173	0.283
ST	n.p.	1.674	0.210	1216	8.344	n.p.	n.p.	1.832	0.411	n.p.	1.374	0.406
OR	n.p.	0.782	0.217	1.248	1.14	0.236	0,209	5.04	0.61	n.p.	1.627	0.141
BO	n.p.	n.p.	n.p.	n.p.	n.p.	n.p.	n.p.	0.045	0.122	1.374	1.707	0.868
SA	n.p.	0.709	0,246	1386	0.569	0.314	n.p.	1.661	0.678	n.p.	4.056	0.288
P1	n.p.	1.34	0.179	1420	0.816	0.266	n.p.	3.694	0.864	2.096	2.725	n.p.
LC	n.p.	1.22	0,171	1.327	0.653	0.439	n.p.	1.146	0.613	2.013	2.157	0.653
CV	n.p.	1.23	0,216	1062	0.702	0.290	n.p.	1.022	0.427	1.607	1.727	0.431
CS	0.215	0.989	0.427	1229	0.711	0.239	0.152	1.684	0.637	1.484	1.679	0.188

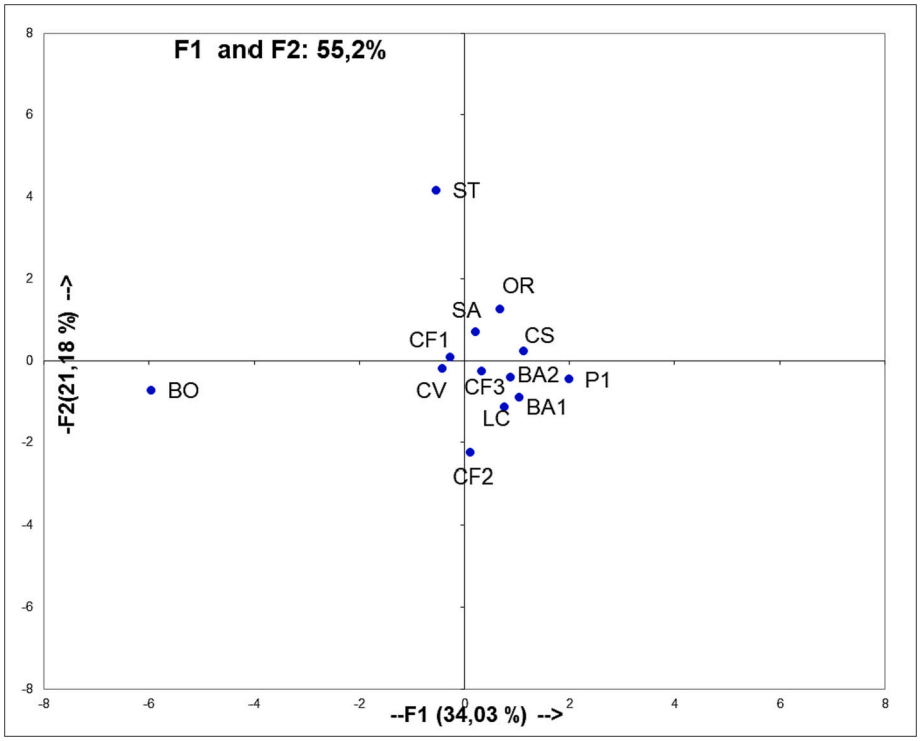

Fig. 6. Scatter plot obtained from the plastitar samples considering the geochemical indicators.

some of the highest reported values for coastal environments in the Mediterranean basin, suggesting that tar is effectively acting as a plastic accumulator. For instance, Vianello et al. (2013) reported a maximum concentration of 1400 particles/kg in sandy beaches of the Venice lagoon. Because statistical analysis did not highlight any significant difference in the plastic concentration retrieved from different locations (likely due to the high variance displayed by replicates collected from the same location), it can be assumed that the occurrence of plastic in the plastitar mats deposited onto the coastline follow the typical patchy distribution that was already underlined for plastic accumulation in coastal environments (Chubarenko et al., 2020). During our survey, a number of tarballs were also observed along the shoreline, however these were found to not contain plastic at all and were not considered in this study since the aim of our investigation was the identification and chemical characterization of plastitar in the Mediterranean Sea. Both in our study as well as in the study of Domínguez-Hernández et al. (2022), the frequency of plastic contamination in tar residues was not considered, but clearly this topic must be covered by future studies, also considering the gap in the historical record of tar and plastic interactions.

As we highlighted in the results section, the distribution of admixed plastic particles in the tar mat was not homogeneous and significant differences were found between the outer surface and the inner core. Depth gradients and marked differences were also found in the accumulation of different particle shapes within the tar matrix. This observation suggests that the processes involved in the plastitar genesis are in some way comparable among different locations and ultimately related to the specific mechanism of plastitar formation. Segregation of particles under different fragmentation and transport mechanisms have been already reported in the plastic pollution literature. For instance, a study carried out in the Canary Islands that considered plastic accumulation on different beaches by sediment coring highlighted how plastic particles tend to preferentially accumulate in high tide sediment than in submerged sediment (Reinold et al., 2021). In our Mediterranean samples, we found a relatively high occurrence of plastic pellets on the plastitar surface, with nurdles representing 46 % of the total particles detected in the outer tar layers. The literature generally indicates that pellets only represent 2.2 % of all plastic particles retrieved in Mediterranean surface waters (Suaria et al., 2016) and 5.6 % of the plastic items retrieved from Adriatic coastal beaches (Munari et al., 2017). Similarly, in Mediterranean beaches, a concentration of 1.2 ± 2 pellets per kg of sediment was reported by Piperagkas et al. (2019). The pellet concentration found in our samples must be considered exceptionally high and should be related to some peculiar mechanism of association occurring during the plastitar genesis. Similarly, the fact that lines and filaments were found to be prevalent in the inner layers of the plastitar formations pose some interesting questions that deserve to be carefully considered. Both lines and nurdles are mostly composed by PE and PP. The prevalence of polyolefins is in line with what has been previously reported in plasticrusts, pyroplastics and other novel geological formations (Ehlers and Ellrich, 2020; Ehlers et al., 2021). Authors indicated in this case that the main origin of PE lines may be associated with maritime ropes scouring across raspy rocks and being melted due to high surface temperature of rocks during summer. We believe that a similar mechanism may explain the admixing of lines and nurdles in the inner core of the tar material. However, since we did not find melted ropes in our samples, we can hypothesize that the immobilization of the materials in the viscous matrix of the tar mat, may prevent their further degradation.

As described by Domínguez-Hernández et al. (2022), the formation of plastitars on the rocky shore may be occurring through an initial stranding onto the rocky shore of oily residues carried out by strong currents and storms that during the daily exposition to UV light and warm temperatures ultimately hardening the material. The mixing of the plastic fragments settled by tides occurs therefore in a second stage of the process, that starts necessarily after oil deposition on the rocky shore. During the evaporation of the lightweight and volatiles components of the tar and the solidification of its high molecular weight fraction, a solid structure is ultimately formed and sticks to the coastal rocks, agglomerating in the meanwhile the variety of materials such as wood, glass, sand and plastics that come in contact due to tide and waves. The hardening process of the petroleum residues is widely

described in the literature to explain tar coastal pollution, this process is chemically related to the weathering process that involves evaporation, dissolution, dispersion, water–oil emulsification, microbial degradation, photooxidation, adsorption onto suspended particulate materials, and oil–mineral aggregation (Bragg and Owens, 1994).

As noted in the previous section, the current high level of plastic pollution is probably the main reason why tar is now found admixed to plastic: when the oil is stranded it enters in contact with plastic that is readily admixed in the viscous and pliable matrix, and then remains stuck after hardening of the material. In our observation, we noticed how floating debris (see picture in the supplementary file) just layered from the tide on the top of an already hardened plastitar sample. These plastic items did not get admixed to the plastitar surface when already consolidated. Moreover, we had the chance to examine a tar residue carried out by the sea on a rocky costal area, stranding with no plastic admixed. Both these observations suggests that the admixing of plastic to tar may require a specific timing (plastic are layered by the tide before the tar starts the hardening process). On the other hand, it cannot be excluded that the plastic and tar might be collected together by surface currents before stranding (so we may infer "a fast plastitar formation" process). Interestingly, we also found a sample in a sandy beach (sample CS in Table 1), which was strongly different in appearance from the tar mat retrieved on the rocky coast, presenting a rounded and stony shape with similar textural characteristics of natural debris, most likely due to a transport mechanism resembling the sedimentary transport. As discussed by Corcoran and coauthors (Corcoran et al., 2014; Corcoran and Jazvac, 2020), this new "rock type" presence in the marine environment open a debate about the signs of Anthropocene in the marine geological environment, since this material are not rocks considering that rocks are formed "naturally", whereas these novel items are composed of anthropogenic products (plastic) shaped both by anthropogenic and natural processes or actions, and natural sedimentary clasts may withstand breakage and weathering (in some cases even more than the natural counterpart). Moreover, this material, besides plastic, accumulates pieces of wood or coarse sand grains as well as small rocks, thus creating a new signature of the conjunction between natural and man-made materials in the environment.

4.2. *Information from the geochemical indicators*

Petroleum is a complex mixture of thousands of different organic compounds formed from a variety of organic materials that are chemically converted under differing geological conditions over long periods of time under a collection of different diagenetic and catagenitic processes (Wang and Fingas, 2003). The current commercially available petroleum products used from vehicles traction to lubricants are in fact refined fractions of these "natural petroleums", obtained after the application of industrial distillation. These products may ultimately present the occurrence of distinct chemical profiles that are caused both by the variability in the original feedstock source and by the different refinery process applied. The differences in the chemical compositions that crude oils and petroleum products display are the main basis for their "fingerprinting" and "provenancing". The general process leading to the accumulation of tar on the shoreline is widely described in the scientific literature. As already mentioned in the previous sections, this process involves spreading and evaporation of petroleum residues that occurs at the very beginning of the weathering process, followed by dissolution, biodegradation, photooxidation, emulsification and sedimentation. Forced by these processes both the physical and chemical properties of the spilled oil may be altered significantly. For instance, during weathering alkanes and isoprenoids may disappear. Lighter aromatic hydrocarbons (BTEX, some lightweight PAH compounds such as naphthalene and lightweight alkyl-benzenes) that are more soluble than high molecular weight and alkylated aromatics hydrocarbons, and also of aliphatic hydrocarbons, are easily lost by "water-washing" and rarely observed in tar residues. Literature indicates that in some instances, the oil profile may result also too weathered to attempt any classification on the basis of the TIC profile, fundamentally due to the removal of n-alkanes and other compounds, resulting in a large and unresolved complex mixture (UCM). On the other hand, the literature also reports several attempts of differentiating between natural and anthropogenic petroleum sources of tar material retrieved in the coastal environment, by the application geochemical markers that can withstand the chemical alterations caused by weathering (Wang and Fingas, 2003). For this challenge, a large variety of analytical approaches has been developed to recognize crude oils imported by tankers from local production wells, and to evaluate seasonal transport and distribution patterns.

Fingerprinting by ratios of the molecular constituents were shown to effectively enable the discrimination between different tarballs transported far from their source by ocean currents and to tentatively identify the original seepage. For instance, it was shown that it is possible to discriminate among different tarballs that have been transported far from their sources by ocean currents and found also a correlation with natural seeps (Page et al., 1999). Especially during the Exxon Valdez oil spill in Prince William Sound (Alaska), various analytical approaches to obtain hydrocarbon fingerprints have been developed and validated (Boehm et al., 1997; Page et al., 1999). There are also evidences that after a spill, the chemical characteristic of the oil may be retained unaltered, especially when the spilled oil is retained in subsurface waters in anaerobic conditions and cold temperatures. For instance, during the Nipisi spill authors showed how oil samples collected over a 25-years' time span displayed the same n-alkane, alkylated benzene and alkylated PAH profiles (Wang et al., 1998). Ultimately, a proper knowledge regarding the mechanics of the hydrocarbon formation in the shallow seeps and of the transport from the marine environment onto the shore is lacking, hence it is currently not possible to provide irrefutable data linking stranded oils residues to specific offshore natural seeps (Leifer et al., 2004).

In our survey, none of the samples displayed a lack of diagnostics feature and overall, marked differences among all samples could be appreciated both considering the morphological features as well as their chemical profiles. The tar residues displayed a wide variety of morphologies from the classical solid rock consistency with conchoidal fracturing of asphaltites, to the sticky and deformable behavior of the tar residues, suggesting a highly heterogeneous provenance of the tar fractions. SARA and CHN/S analysis confirmed a high heterogeneity in the chemical composition, with marked differences in the heteroatoms contents (especially the sulfur) and in the asphaltenes relative concentration. Geochemical parameters were found to vary among all the samples, with most of the samples displaying high values of thermal maturity but indication of different seep provenance from deep sea to surficial seeps, and with different diagenetic and catagenetic processes involved origin (since the geochemical indicators surveyed are usually applied to the discrimination of marine and terrestrial source of petroleum and of the rock influenced catagenesis). Also, multivariate statistical analysis confirmed a clear differentiation of our sample set on the basis of their geochemical parameters.

Considering the high heterogeneity of the recorded chemical profiles, it is likely that some of the tar residues surveyed in our study are not related to natural Mediterranean seeps, but they most probably originated from accidental spills or unregulated tank washings caused by maritime traffic. Any attempts for a more precise source recognition are currently infeasible. Samples CS, CF1, BA1, BA2, P1 and SA showed the typical bimodal profile of bunker oil. P1 and SA showed also the presence of man-made additives such as acrylates. Samples CF2 and CF3 showed a trimodal distribution that may be explained by considering that bunker fuels are often obtained by blending residual oils with diesel fuels or other lighter fuels in various ratios. Of course, the blending may lead to substantial variation of their geochemical parameters, and this may explain some contradictory indications regarding maturity and source provided by the different indicators. Of course, some of the residues may also have a natural origin since in the Mediterranean Sea the

occurrence of natural seepage is widely documented (Rovere et al., 2017). Italy for instance, hosts the largest natural petroleum systems in southern Europe, with about 60 fields in active production. The occasional release of liquid hydrocarbons has been already hypothesized, but it has been also highlighted that at present, the occurrence of this phenomena is still poorly monitored (Rovere et al., 2017). In the clay-poor calcareous rocks of the Adriatic Sea, diasteranes were reported to occur in high levels (Moldowan et al., 1991). Again, since we did not find diasteranes in the samples retrieved from the Salento coast (our only Adriatic sample), this may prove the absence of a direct link between the natural seep and that the most likely source of this tar was an oil spill.

4.3. Plastitar, a coastal sink for plastic debris?

In their paper, Domínguez-Hernández et al. (2022) reported that they had the chance to follow the accumulation of plastitar on a costal rock in real time: firstly, they noted during a microplastic sampling campaign the arrival of large amounts of tar residues along the beaches of Arenas Blancas and Playa Grande in the Canary Islands. They observed how the stranded material ultimately stuck to the rocks surface and during time it agglomerated the other materials brought to the shore by the sea and mixed them with tar. From this experience, the authors suggested that the day-night solar irradiation cycle causing a cyclic hardening and softening of the material may be the major driver of the progressive inclusion of foreign plastic particles and their subsequent immobilization into the tar structure. During our surveys, we had the chance to witness a very similar process. In the southern coast of Salento (Supplementay Material, Section S1), we observed the stranding of a tar residue without plastic on a local rocky shore. In the following weeks we observed how this residue was getting in close contact with plastic debris due to the waves and tide action. However, in our experience, plastitar formation may also follow other pathways. For instance, in Sardinia, we found plastitar accumulated underwater (approx. 2–5 m below sea level, Supplementary material, Section S1), thus indicating that the role of daily UV-light cycle after stranding might be less relevant than other factors inducing the hardening of the material before stranding (i.e., water turbulence, UV light exposition during transport at the sea surface, wave action, water temperature). A second interesting observation is that two-locations that we surveyed annually for 5 years (Calavinagra and Memmerosso in San Pietro Island, Sardinia), did not show relevant variations in the tar distribution on the rocky coastal surface. Plastitar formations were already present at the first visit, and remained pretty much constant for 5 years, suggesting that the hardening and plastic incorporation process occurred only once when the plastitar was formed. Interestingly, new microplastics carried out by stormy conditions and layered on the top of the already hardened material, were not incorporated in the tar, most likely because the consolidation of the external layer prevented them to be admixed (see Supplementary Section 3 Fig. S3). We also observed the occurrence of moving bed biofilm reactors (MBBR) layered on the top of plastitar and not admixed to the plastitar (Supplementary material, section S1). This observation may be considered as a hint that the hardening of the material preventing plastic admixing may be also used to date back the tar accumulation (and at the same time that the tar behave as an archive of historical plastic pollution events) since the contamination of MMBRs in the Mediterranean sea is thought to be related to a large spill event occurred in 2018 from a wastewater treatment plant in the Sele river, in the Thyrrenian sea (Redazione-ANSA, 2018). Most of the lines and ropes accumulated in the inner surface of the tar, while plastic nurdles were more common on the top. This observation seems to suggest that the tar mat is capable of both inducing a segregation of the different plastic items and also preserving them to some extent from further fragmentation, essentially preventing further thermal and mechanical stress on the rock surface (Ehlers et al., 2021), contrarily to what was reported for plastic-rock complexes by Wang et al. (2023). From this point of view, the adhesion to the sticky matrix of the tar mat may in some way reduce the mechanical stress and thus render the tar a sink for plastic preservation that may ultimately work as an archive of historical plastic debris. We further empirically confirmed this, since in the Southern Adriatic, we found admixed to the viscous matrix, very old plastic items (named 'Archeoplastics') which were dated back to the 1950s–1970s thanks to their labels and shape. For related images please check Supplementary section S1 of this paper and the related web page (https://www.archeoplastica.it/).

Finally, considering that the Mediterranean Sea represents one of the most important hotspots of terrestrial and marine biodiversity (Coll et al., 2010), hosting about 7 % of the world's marine species with many local overlooked habitats, including endemic and protected species (Bianchi and Morri, 2000; Micaroni et al., 2022; Grech et al., 2020) and that tar contains high levels of polycyclic aromatic hydrocarbons and plastics are capable to cause adverse health effects for marine organism (Gall and Thompson, 2015; Honda and Suzuki, 2020) actions are strongly required to further limit the spills of plastics and other petroleum related products in the marine environment and prevent their impacts onto marine ecosystems.

5. Conclusion

In conclusion, this study confirmed that plastitar formations are common and widespread in the Mediterranean Sea. The geochemical profile of the tar fraction revealed heterogeneous seep origins and key distinctive features in the plastic distribution within the tar mat layers were also highlighted. A prevalence of plastic pellets (nurdles) in the external layers and the occurrence of well-preserved lines and ropes in the inner layers was observed. Based on our observations, we suggest that the tar stranded on the coastal shores, regardless of its origin (natural seeps or accidental oil spills from commercial vessels), is currently acting as sink for plastic debris, storing and preserving plastic from degradation, and also providing an historical archive of pollution events.

CRediT authorship contribution statement

Francesco Saliu: *Conceptualization; Investigation; Data curation; Writing – original draft and revision.*

Montserrat Compa *Resources*, *writing original paper.*

Alessandro Becchi *GC–MS analyis.*

Marina Lasagni *Project administration.*

Elena Collina *Funding acquisition;*

Arianna Liconti *Resources*, *sampling in Ligurian Sea.*

Enzo Suma *Resources*, Sampling in Adriatic Sea.

Salud Deudero *Resources*, *writing original paper*, *Sampling in Western Mediterranean.*

Daniele Grech, *Resources*, *writing original paper*, *Sampling in Sardinia.*

Giuseppe Suaria *Investigation; Resources*, *writing original paper.*

Declaration of competing interest

The authors declare that they have no known competing financial interests or personal relationships that could have appeared to influence the work reported in this paper.

Data availability

Data will be made available on request.

Acknowledgements

We warmly thank Andrea Ghitti for the precious help in running the experimental work by GC–MS.

Funding for this research was obtained through the following projects: EU-funded Interreg Med Plastic Busters MPAs project: preserving

biodiversity from plastics in Mediterranean Marine Protected Areas (co-financed by the European Regional Development Fund; grant number: 4MED17_3.2_M123_027). PRIN-EMME Exploring the fate of Mediterranean microplastics: from distribution pathways to biological effects (contract number: 2017WERYZP). EUROqCHARM - "EUROpean quality ControlledHarmonization Assuring Reproducible Monitoring and assessment of plastic pollution" (grant agreement: 101003805). This output reflects only the author's view and the European Union cannot be held responsible for any use that may be made of the information contained therein.

Appendix A. Supplementary data

Supplementary data to this article can be found online at https://doi.org/10.1016/j.marpolbul.2023.115583.

References

Bence, A.E., Kvenvolden, K.A., Kennicutt II, M.C., 1996. Organic geochemistry applied to environmental assessments of Prince William Sound, Alaska, after the Exxon Valdez oil spill— a review. Org. Geochem. 24, 7–42.

Bianchi, C.N., Morri, C., 2000. Marine biodiversity of the Mediterranean Sea: situation, problems and prospects for future research. Mar. Pollut. Bull. 40, 367–376.

Boehm, P.D., Douglas, G.S., Burns, W.A., Mankiewicz, P.J., Page, D.S., Bence, A.E., 1997. Application of petroleum hydrocarbon chemical fingerprinting and allocation techniques after the Exxon Valdez oil spill. Mar. Pollut. Bull. 34, 599–613.

Bragg, J.R., Owens, E.H., 1994. Clay-oil flocculation as a natural cleansing process after oil spills: Part 1: Studies of shoreline sediments and residues from past spills. In: Proceedings of the 17th Arctic and Marine Oil Spill Program (AMOP) Technical Seminar, Vancouver, British Columbia, pp. 1–24.

Christensen, L.B., Larsen, T.H., 1993. Method for determining the age of diesel oil spills in the soil. Ground Water Monit. Remediat. Fall 142–149.

Chubarenko, I., Esiukova, E., Khatmullina, L., Lobchuk, O., Grave, A., Kileso, A., Haseler, M., 2020. From macro to micro, from patchy to uniform: analyzing plastic contamination along and across a sandy tide-less coast. Mar. Pollut. Bull. 156, 111198.

Coll, M., Piroddi, C., Steenbeek, J., Kaschner, K., Lasram, F.B.R., Aguzzi, J., Ballesteros, E., Bianchi, C.N., Corbera, J., Dailianis, T., Danovaro, R., et al., 2010. The biodiversity of the Mediterranean Sea: estimates, patterns, and threats. PLoS One 5, e11842.

Corcoran, P.L., Jazvac, K., 2020. The consequence that is plastiglomerate. Nat. Rev. Earth Environ. 1 (1), 6–7.

Corcoran, P.L., Moore, C.J., Jazvac, K., 2014. An anthropogenic marker horizon in the future rock record. GSAT 4–8.

Corrick, A.J., Hall, P.A., Gong, S., McKirdy, D.M., Trefry, C., Ross, A.S., 2021. The characterisation and provenance of crude oils stranded on the South Australian coastline. Part I: Oil types and their weathering. Mar. Pollut. Bull. 167, 112260.

Crain, C.M., Kroeker, K., Halpern, B.S., 2008. Interactive and cumulative effects of multiple human stressors in marine systems. Ecol. Lett. 11 (12), 1304–1315.

Crawford, C., Quinn, B., 2017. Plastic production, waste and legislation. Micro. Pollut. 11, 39–56. https://doi.org/10.1016/B978-0-12-809406-8.00003-7.

Curiale, J.A., Cameron, D., Davis, D.V., 1985. Biological marker distribution and significance in oils and rocks of the Monterey Formation, California. Geochim. Cosmochim. Acta 49, 271–288.

De-la-Torre, G.E., Dioses-Salinas, D.C., Pizarro-Ortega, C.I., Santillán, L., 2021. New plastic formations in the Anthropocene. Sci. Total Environ. 754, 142216.

De-la-Torre, G.E., Pizarro-Ortega, C.I., Dioses-Salinas, D.C., Rakib, M.R.J., Ramos, W., Pretell, V., Ribeiro, V.V., Castro, Í.B., Dobaradaran, S., 2022. First record of plastiglomerates, pyroplastics, and plasticrusts in South America. Sci. Total Environ. 833, 155179.

Domínguez-Hernández, C., Villanova-Solano, C., Sevillano-González, M., Hernández-Sánchez, C., González-Sálamo, J., Ortega-Zamora, C., Díaz-Peña, F.J., Hernández-Borges, J., 2022. Plastitar: a new threat for coastal environments. Sci. Total Environ. 839, 156261.

Ehlers, S.M., Ellrich, J.A., 2020. First record of 'plasticrusts' and 'pyroplastic' from the Mediterranean Sea. Mar. Pollut. Bull. 151, 110845.

Ehlers, S.M., Ellrich, J.A., Gestoso, I., 2021. Plasticrusts derive from maritime ropes scouring across raspy rocks. Mar. Pollut. Bull. 172, 112841.

Ensminger, A., van Dorsselaer, A., Spykerelle, C., Albrecht, P., Ourisson, G., 1974. Pentacyclic triterpanes of the hopane type as ubiquitous geochemicalmarkers-origin and significance. In: Tissot, B., Brenner, F. (Eds.), Advances in Organic.

Eriksen, M., Cowger, W., Erdle, L.M., Coffin, S., Villarrubia-Gómez, P., Moore, C.J., Carpenter, E.J., Day, R.H., Thiel, M., Wilcox, C., 2023. A growing plastic smog, now estimated to be over 170 trillion plastic particles afloat in the world's oceans—urgent solutions required. PLoS One 18 (3), e0281596.

Galgani, F., Hanke, G., Werner, S., De Vrees, L., 2013. Marine litter within the European marine strategy framework directive. ICES J. Mar. Sci. 70 (6), 1055–1064. https://doi.org/10.1093/icesjms/fst122.

Gall, S.C., Thompson, R.C., 2015. The impact of debris on marine life. Mar. Pollut. Bull. 92, 170–179.

Gestoso, I., Cacabelos, E., Ramalhosa, P., Canning-Clode, J., 2019. Plasticrusts: a new potential threat in the Anthropocene's rocky shores. Sci. Total Environ. 687, 413–415.

Goswami, P., Bhadury, P., 2023. First record of an Anthropocene marker plastiglomerate in Andaman Island, India. Mar. Pollut. Bull. 190, 114802.

Grech, D., Van De Poll, B., Bertolino, M., Rosso, A., Guala, I., 2020. Massive stranding event revealed the occurrence of an overlooked and ecosystem engineer sponge. Mar. Biodivers. 50, 82.

Honda, M., Suzuki, N., 2020. Toxicities of polycyclic aromatic hydrocarbons for aquatic animals. IJERPH 17, 1363.

Hostettler, F.D., Rosenbauer, R.J., Kvenvolden, K.A., 1999. PAH refractory index as a source discriminant of hydro carbon input from crude oil and coal in Prince William sound, Alaska. Org. Geochem. 30, 873–879.

Hostettler, F.D., Rosenbauer, R.J., Lorenson, T.D., Dougherty, J., 2004. Geochemical characterization of tarballs on beaches along the California coast. Part I—shallow seepage impacting the Santa Barbara Channel Islands, Santa Cruz, Santa Rosa and San Miguel. Org. Geochem. 35 (6), 725–746.

Kaplan, I.R., Galperin, Y., Lu, S., Lee, R.P., 1997. Forensic environmental geochemistry differentiation of fuel-types, their sources, and release time. Org. Geochem. 27, 289–317.

Kovats, E., 1958. Gas-chromatographische Charakterisierung organischer Verbindungen. Teil 1: Retentionsindices aliphatischer Halogenide, Alkohole, Aldehyde und Ketone. Helv. Chim. Acta 41, 1915–1932.

Kvenvolden, K.A., Rosenbauer, R.J., Hostettler, F.D., Lorenson, T.D., 2000. Application of organic geochemistry to coastal tar residues from Central California. Int. Geol. Rev. 22, 1–14.

Leifer, I., Boles, J.R., Luyendyk, B.P., Clark, J.F., 2004. Transient discharges from marine hydrocarbon seeps: spatial and temporal variability. Environ. Geol. 46 (8), 1038–1052.

Mackenzie, A.S., 1984. Applications of biological markers in petroleum geochemistry. In: Brooks, J., Welte, D. (Eds.), Advances in Petroleum Geochemistry, vol. 1. Academic Press, London, pp. 115–214.

Martí, E., Martin, C., Galli, M., Echevarría, F., Duarte, C.M., Cózar, A., 2020. The colors of the ocean plastics. Environ. Sci. Technol. 54, 6594–6601.

Micaroni, V., Strano, F., Crocetta, F., Di Franco, D., Piraino, S., Gravili, C., Rindi, F., Bertolino, M., Costa, G., Langeneck, J., Bo, M., Betti, F., Froglia, C., Giangrande, A., Tiralongo, F., Nicoletti, L., Medagli, P., Arzeni, S., Boero, F., 2022. Project "biodiversity MARE tricase": a species inventory of the coastal area of southeastern Salento (Ionian Sea, Italy). Diversity 14, 904.

Moldowan, J.M., Fago, F.J., Carlson, R.M.K., Young, D.C., Duvne, G., Clardy, J., Schoell, M., Pillinger, C.T., Watt, D.S., 1991. Rearranged hopanes in sediments and petroleum. Geochim. Cosmochim. Acta 55 (11), 3333–3353. https://doi.org/10.1016/0016-7037(91)90492-N.

Munari, C., Scoponi, M., Mistri, M., 2017. Plastic debris in the Mediterranean Sea: types, occurrence and distribution along Adriatic shorelines. Waste Manag. 67, 385–391.

Page, D.S., Boehm, P.D., Douglas, G.S., Bence, A.E., Burns, W.A., Mankiewicz, P.J., 1999. Pyrogenic PAHs in sediments record past human activity: a case study in Prince William Sound. Alaska Mar. Pollut. Bull. 38 (4), 247–260.

Palacas, J.G., Anders, D.E., King, J.D., 1984. South Florida Basin— a prime example of carbonate source rocks of petroleum. In: Palacas, J.G. (Ed.), Petroleum Geochemistry and Source Rock Potential of Carbonate Rocks. American Association of Petroleum Geologists, pp. 71–96. Studies in Geology No. 18.

Peters, K.E., Moldowan, J.M., 1993. The Biomarker Guide. Prentice Hall, Englewood Cliffs, New Jersey, 363 pp.

Piperagkas, O., Papageorgiou, N., Karakassis, I., 2019. Qualitative and quantitative assessment of microplastics in three sandy Mediterranean beaches, including different methodological approaches. Estuar. Coast. Shelf Sci. 219, 169–175.

Rangel-Buitrago, N., Neal, W., Williams, A., 2022. The Plasticene: time and rocks. Mar. Pollut. Bull. 185, 114358.

RedazioneANSA, 2018. ROMA 20. marzo. https://www.ansa.it/canale_ambiente/notizie/inquinamento/2018/03/20/dischetti-ministero-vengono-da-container-o-depuratore_2144059d-d5fb-45ed-8d00-798f6e3e36b7.html.

Reinold, S., Herrera, A., Stile, N., Saliu, F., Hernández-González, C., Zaida Ortega, I.M., Marrero, M.D., Lasagni, M., Gómez, M., 2021. An annual study on plastic accumulation in surface water and sediment cores from the coastline of Tenerife (Canary Island, Spain). Mar. Pollut. Bull. 173, 113072.

Rovere, M., Campiani, E., Leidi, E., Mercorella, A., 2017. Natural hydrocarbon seepage in the Italian offshore. Geoing. Ambient. Min. 35–40.

Saliu, F., Montano, S., Garavaglia, M.G., Lasagni, M., Seveso, D., Galli, P., 2018. Microplastic and charred microplastic in the Faafu Atoll, Maldives. Mar. Pollut. Bull. 136, 464–471.

Saliu, F., Lasagni, M., Andò, S., Ferrero, L., Pellegrini, C., Calafat, A., Sanchez Vidal, A., 2023. A baseline assessment of the relationship between microplastics and plasticizers in sediment samples collected from the Barcelona continental shelf. Environ. Sci. Pollut. Res. 30, 36311–36324.

Santos, F.A., Diório, G.R., Guedes, C.C.F., Fernandino, G., Giannini, P.C., Angulo, R.J., de Souza, M.C., César-Oliveira, M.A.F., dos Santos Oliveira, A.R., 2022. Plastic debris forms: rock analogues emerging from marine pollution. Mar. Pollut. Bull. 182, 114031.

Seifert, W.K., Moldowan, J.M., 1978. Application of steranes, terpanes, and monoaromatics to the saturation, migration and source of crude oils. Geochim. Cosmochim. Acta 42, 77–95.

Shiber, J.G., 1987. Plastic pellets and tar on Spain's Mediterranean beaches. Mar. Pollut. Bull. 18 (2), 84–86.

Shiber, J.G., 1989. Plastic particle and tar pollution on beached of Kuwait. Environ. Pollut. 57 (4), 341–351.

Shiber, J.G., Barralesrienda, J.M., 1991. Plastic pellets, tar, and megalitter on Beirut beaches, 1977–1988. Environ. Pollut. 71 (1), 17–30.
Suaria, G., Avio, C.G., Mineo, A., Lattin, G.L., Magaldi, M.G., Belmonte, G., Moore, C.J., Regoli, F., Aliani, S., 2016. The Mediterranean plastic soup: synthetic polymers in Mediterranean surface waters. Sci. Rep. 6, 37551.
Turner, A., Holmes, L., 2011. Occurrence, distribution and characteristics of beached plastic production pellets on the island of Malta (central Mediterranean). Mar. Pollut. Bull. 62 (2), 377–381.
Turner, A., Wallerstein, C., Arnold, R., Webb, D., 2019. Marine pollution from pyroplastics. Sci. Total Environ. 694, 133610. https://doi.org/10.1016/j.scitotenv.2019.133610.
Venkatesan, M.I., 1988. Occurrence and possible sources of perylene in marine sediments—a review. Mar. Chem. 25, 1–27.
Vianello, A., Boldrin, A., Guerriero, P., Moschino, V., Rella, R., Sturaro, A., Da Ros, L., 2013. Microplastic particles in sediments of Lagoon of Venice, Italy: first observations on occurrence, spatial patterns and identification. Estuar. Coast. Shelf Sci. 130, 54–61.
Wang, L., Bank, M.S., Rinklebe, J., Hou, D., 2023. Plastic-rock complexes as hotspots for microplastic generation. Environ. Sci. Technol. 57 (17), 7009–7017.
Wang, Z., Fingas, M., 2003. Development of oil hydrocarbon fingerprinting and identification techniques. Mar. Pollut. Bull. 47 (2003), 423–452.
Wang, Z., Stoutt, S.A., Fingas, M., 2006. Environmental Forensics, 7. CopyrightC©Taylor & Francis Group, pp. 105–146. https://doi.org/10.1080/15275920600667104. LLCISSN: 1527–5922 print/1527–5930 online. (Forensic Fingerprinting of Biomarkers for Oil Spill Characterization and Source Identification).
Wang, Z.D., Fingas, M., Blenkinsopp, S., Sergy, G., Landriault, M., Sigouin, L., 1998. Study of the 25-year-old Nipisi oil spill: persistence of oil residues and comparisons between surface and subsurface sediments. Environ. Sci. Technol. 32 (15), 2222–2232.
Zalasiewicz, J., Waters, C.N., Ivar do Sul, J.A., Corcoran, P.L., Barnosky, A.D., Cearreta, A., Edgeworth, M., Gałuszka, A., Jeandel, C., Leinfelder, R., McNeill, J.R., Steffen, W., Summerhayes, C., Wagreich, M., Williams, M., Wolfe, A.P., Yonan, Y., 2016. The geological cycle of plastics and their use as a stratigraphic indicator of the Anthropocene. Anthropocene 13, 4–17. https://doi.org/10.1016/j.ancene.2016.01.002.